

# MBA: Multimodal Bidirectional Attack for Referring Expression Segmentation Models

Xingbai Chen<sup>a</sup>, Tingchao Fu<sup>a</sup>, Renyang Liu<sup>c</sup>, Wei Zhou<sup>a,b</sup>, Chao Yi<sup>a</sup>

<sup>a</sup>National Pilot School of Software, Yunnan University, Kunming, 650504, Yunnan, China

<sup>b</sup>School of Information Science and Engineering, Yunnan University, Kunming, 650504, Yunnan, China

<sup>c</sup>Institute of Data Science, National University of Singapore, Singapore, 117602, Singapore

---

## Abstract

Referring Expression Segmentation (RES) enables precise object segmentation in images based on natural language descriptions, offering high flexibility and broad applicability in real-world vision tasks. Despite its impressive performance, the robustness of RES models against adversarial examples remains largely unexplored. While prior adversarial attack methods have explored adversarial robustness on conventional segmentation models, they perform poorly when directly applied to RES, failing to expose vulnerabilities in its multimodal structure. Moreover, in practical open-world scenarios, users typically issue multiple, diverse referring expressions to interact with the same image, highlighting the need for adversarial examples that generalize across varied textual inputs. To address these multimodal challenges, we propose a novel adversarial attack strategy termed **Multimodal Bidirectional Attack**, tailored for RES models. Our method introduces learnable proxy textual embedding perturbation and jointly performs visual-aligned optimization on the image modality and textual-adversarial optimization on the textual modality during attack generation. This dual optimization framework encourages adversarial images to actively adapt to more challenging text embedding during optimization, thereby enhancing their cross-text transferability, which refers to the ability of adversarial examples to remain effective under a variety of unseen or semantically diverse textual inputs. Extensive experiments conducted on multiple RES models and benchmark datasets demonstrate the superior effectiveness of our method compared to existing methods. Furthermore, considering the privacy protection scenario, our approach effectively restricts RES models from extracting sensitive content in personal images without explicit authorization, thereby contributing to the understanding of robustness and security in multimodal vision-language systems.

*Keywords:* Adversarial Attack, Adversarial Robustness, Referring Expression Segmentation, Model Vulnerability, Deep Learning

---

## 1. Introduction

Image segmentation is a fundamental task in computer vision, aiming to assign semantic labels to pixels and delineate object boundaries. With deep learning, models such as [1, 2, 3] have greatly improved segmentation performance. Building on this progress, Referring Expression Segmentation (RES) [4, 5, 6, 7, 8, 9] enables language-guided segmentation and has shown notable success. This task combines natural language processing with visual understanding, enabling users to specify target objects in an image through natural language descriptions, thereby supporting more flexible and intelligent segmentation. Although significant progress has been made in improving segmentation accuracy and generalization in recent years, the robustness of RES models against adversarial examples [10, 11], which are inputs perturbed with imperceptible but carefully crafted noise to mislead the model into making incorrect predictions, remains largely unexplored. While previous research [12, 13] has extensively investigated the vulnerability of traditional segmentation models to such attacks, existing methods perform poorly when applied to RES models and fail to reveal the risks inherent in their unique multimodal architectures. Therefore, a comprehensive investigation

---

*Email addresses:* chenxingbai@stu.ynu.edu.cn (Xingbai Chen), futingchao@stu.ynu.edu.cn (Tingchao Fu), ryliu@nus.edu.sg (Renyang Liu), zwei@ynu.edu.cn (Wei Zhou), yichao@ynu.edu.cn (Chao Yi)

into the adversarial robustness of RES models is imperative, as it enables the identification of vulnerabilities in their vision-language interaction mechanisms while also contributing to the security and reliability of multimodal systems.



Figure 1: Comparison between non-text-based and text-based adversarial attacks on RES models. The top row shows adversarial examples generated by methods that do not consider textual inputs, which fail to consistently suppress segmentation. In contrast, the middle row shows the segmentation predictions for adversarial images generated by our proposed text-based attack, which are explicitly optimized under language conditioning. The bottom row lists the corresponding textual inputs.

Unlike conventional segmentation models [1, 14, 3], RES models inherently involve multimodal interactions between vision and language, which makes exploiting their vulnerabilities substantially more challenging. Attackers must consider not only the visual content but also the diversity of textual provided by user and the semantic interactions between language and vision. Typically, RES models take an image-text pair as input to perform target localization. However, it is often impossible for either attackers or defenders to anticipate how users will construct these image-text pairs in practice. This uncertainty poses substantial obstacles to the design of effective attacks. From the attacker’s perspective, generating adversarial examples that maintain effectiveness across a broad range of textual inputs is critical for achieving consistent deception of RES models through cross-text transferability. From the defender’s perspective, if adversarial perturbations are able to consistently guide the model to produce a predefined target mask such as an all-background mask across a wide range of textual inputs, thereby suppressing its segmentation capabilities, they can function as an effective defense mechanism to prevent RES models from extracting sensitive content from personal images without authorization. In summary, a desired adversarial example should maintain effectiveness under diverse and unseen textual inputs. As illustrated in Fig. 2, this exemplifies the notion of cross-text transferability in RES models. This property is particularly critical for assessing the robustness of RES models in open-world scenarios.

Adversarial attacks [10] are techniques that explore model robustness by misleading predictions through carefully crafted input perturbations. Although adversarial robustness has been extensively studied [12, 15, 16, 17, 18, 19, 20, 13] in segmentation models, there are still notable limitations in the context of RES models. First, most methods [12, 13, 20, 15, 16] for traditional segmentation tasks perturb only a single modality and do not consider the interaction with users. However, in RES tasks, both visual modality and textual modality jointly determine the final prediction. Second, recent studies [19, 18] targeting interactive segmentation models[21] primarily rely on point or box prompts. As shown in Fig. 1, adversarial examples generated based on non-textual prompts cannot be easily transferred to RES models, nor can they generalize across different textual inputs. In summary, these approaches [18, 19, 12, 15, 17, 16, 13] fall short in effectively probing the adversarial robustness of RES models. Therefore, exploring the cross-text transferability of adversarial examples in RES models is of paramount importance, as it not only deepens our

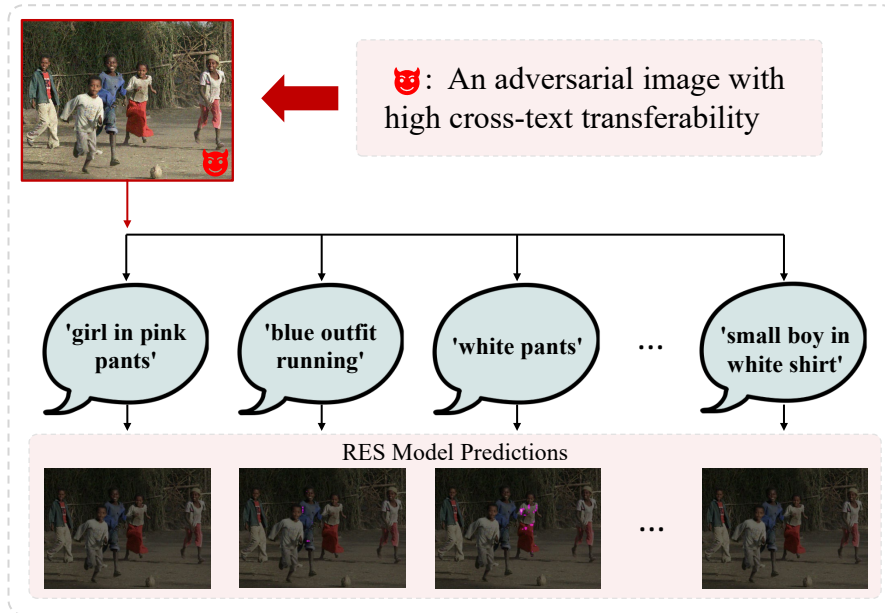


Figure 2: Illustration of a cross-text transferable adversarial image. The adversarial image is designed to mislead the RES model across a wide range of natural language descriptions provided by users. Each textual input refers to the single target object, yet the model consistently fails to generate any segmentation mask. This highlights the potential risk of adversarial examples with strong cross-text generalization in RES tasks.

understanding of their multimodal robustness but also offers new insights for improving the security of such systems.

To overcome the aforementioned limitations and systematically investigate the adversarial robustness of RES models, we propose a novel approach called **Multimodal Bidirectional Attack(MBA)**. This method is designed to enhance the cross-text transferability of adversarial examples by leveraging the multimodal nature of RES models, which jointly process visual and textual inputs for segmentation. Specifically, MBA introduces a dual-stage optimization process. The visual-aligned optimization component focuses on aligning the adversarial image output with a predefined target mask by minimizing the segmentation loss, thereby ensuring that the visual perturbation guides the model toward a specific prediction (e.g., an all-background mask). Meanwhile, during the textual-adversarial optimization phase, we introduce a learnable proxy text embedding perturbation, which serves as a continuous surrogate for the discrete textual input. This design encourages the adversarial image to remain effective under diverse and unseen textual inputs, thereby enhancing its cross-text transferability. This bidirectional optimization strategy mitigates overfitting to proxy texts and enables adversarial examples to generalize across diverse textual inputs, ensuring their effectiveness even when queried with previously unseen referring expressions. Unlike previous methods that either rely on fixed prompts or design without prompt dependence, MBA explicitly models variations in natural language inputs to simulate open-world scenarios, thereby presenting a more realistic and potent adversarial threat. Extensive experiments across multiple RES models and benchmark datasets demonstrate that our method consistently outperforms existing baselines and, more importantly, retains superior effectiveness under previously unseen textual inputs. Our findings not only highlight the latent vulnerabilities of RES models in the textual modality but also offer a new perspective for improving the safety and robustness of multimodal segmentation systems. In brief, our contributions can be summarized as follows:

1. We conduct the first comprehensive study on the adversarial robustness of Referring Expression Segmentation (RES) models, revealing their vulnerability to malicious perturbations in the multimodal setting.
2. We propose a novel attack strategy named *Multimodal Bidirectional Attack(MBA)*. This bidirectional design effectively enhances the cross-text transferability of adversarial examples.
3. We conduct extensive experiments on multiple representative RES models and public benchmark datasets. The results demonstrate that our approach consistently maintains outstanding effectiveness and significantly outperforms existing methods.

## 2. Related Work

### 2.1. Referring Expression Segmentation

RES has emerged as a significant subtask in the field of image segmentation. As a fundamental problem in computer vision, image segmentation aims to assign semantic labels to each pixel by partitioning an image into coherent regions. The rise of deep learning has dramatically advanced this field, with seminal models such as Fully Convolutional Networks (FCN) [2], the DeepLab [3], U-Net [14], and Mask R-CNN [1] greatly improving segmentation accuracy. More recently, foundation models have demonstrated impressive zero-shot generalization capabilities in segmentation tasks. For instance, the Segment Anything Model (SAM) [21], built on Vision Transformers (ViT) [22], supports flexible interactive segmentation through point- and box-based prompts, without being constrained by a fixed category set.

In this context, RES has been proposed to extend traditional category-based segmentation into a language-guided setting. First introduced by [23], RES allows users to specify the target object via natural language expressions, making segmentation more flexible and user-friendly. Unlike conventional segmentation tasks that rely on predefined categories, RES enables free-form object specification through human instructions. Early approaches [24, 25, 26] typically employed convolutional and recurrent neural networks to extract features from visual and linguistic modalities but often struggled to capture the rich cross-modal interactions. To address this limitation, later studies [27, 28, 29] incorporated graph-based reasoning and multimodal relation modeling, significantly enhancing the alignment between language and vision.

With the advent of large-scale vision-language pretraining [30], the capabilities of RES models have seen substantial improvements. Notably, [31] proposed EVF-SAM, which integrates a multimodal encoder [32] into the SAM [21] architecture to support text-prompted segmentation, achieving state-of-the-art performance on various RES benchmarks. Furthermore, the rapid development of large multimodal models [33, 34, 35, 36, 36] has enabled several studies [37, 38, 20] to leverage these pre-trained models for improved language encoding in RES, enhancing generalization in open-domain scenarios.

Despite the promising progress, the adversarial robustness of RES models remains largely unexplored. Given their increasing deployment in real-world applications such as autonomous driving [39], medical image segmentation [40], and human-computer interaction, investigating the vulnerability of RES models under adversarial examples is not only essential for understanding their multimodal decision processes but also critical for ensuring the safety and reliability of vision-language systems.

### 2.2. Adversarial Attack

Adversarial attacks have become a central topic in the study of deep learning security. The Fast Gradient Sign Method (FGSM), introduced by [10], was the first to demonstrate that deep neural networks are highly vulnerable to small, human-imperceptible perturbations intentionally crafted to cause incorrect predictions. Adversarial examples were initially introduced within the domain of image classification, where their primary objective was to deceive models into assigning incorrect labels to input samples.

Adversarial attacks are generally categorized into two types based on the attacker’s knowledge of the model: white-box and black-box attacks. In white-box attacks [10, 11], the attacker has full access to the model’s architecture and parameters. In contrast, black-box attacks [41, 42, 43] operate under the assumption of limited or no access to the target model and primarily rely on either query-based approaches or transfer-based strategies to craft effective adversarial examples.

Beyond classification, researchers have extended adversarial attack techniques to semantic segmentation tasks. One of the earliest efforts in this direction [17] showed that segmentation models are also vulnerable to adversarial perturbations. SegPGD [12] extended the PGD [11] framework by distinguishing between correctly and incorrectly predicted pixels and assigning different optimization weights to these two types, improving attack efficacy. TranSegPGD [13] further advanced this idea by measuring pixel-level cross-model consistency via KL divergence [44], allowing the generation of adversarial examples with stronger cross-model transferability. In addition, several works [15, 45, 46, 47, 16] have explored segmentation robustness from various perspectives, including multi-scale perturbations and adversarial training.

More recently, researchers have begun to investigate adversarial robustness in interactive segmentation models. Attack-SAM [18] is the first attack method tailored to the Segment Anything Model (SAM) [21], which introduced

a prompt-aware loss function and generated adversarial examples guided by user-specified point or box prompts. However, the effectiveness of these examples is limited to the specific prompt used during optimization, and they often fail when evaluated with alternative prompts. To improve generalization across prompts, the SRA (Sampling-based Region Attack) [19] approach proposed a uniform grid-based sampling strategy within the target region, enabling successful attacks regardless of the click location, thereby achieving cross-point prompt attacks.

Despite these advances, existing methods exhibit limited applicability when transferred to RES models. On the one hand, methods developed for traditional segmentation models overlook the role of user input and perform poorly when evaluated under varied textual inputs. On the other hand, attacks designed for point- or box-based interactive models, such as SAM [21], do not naturally extend to RES models that rely on natural language descriptions. Unlike simple point or box prompts, text prompts are inherently more complex and require the model to resolve cross-modal interactions between visual and textual information. Currently, there is no prior work that systematically explores the adversarial robustness of RES models. Given the increasing deployment of RES systems in real-world applications such as autonomous driving, assistive technology, and human-computer interaction, it is crucial to understand their vulnerability to adversarial threats and to develop methods that ensure their reliability in open-world, multimodal environments.

In summary, although prior research has made notable progress in adversarial attacks on conventional and interactive segmentation models, these methods exhibit limited effectiveness when applied to RES models due to their inability to model complex language inputs. Existing segmentation-based attacks often neglect the influence of textual variation, while point- and box-based methods fail to transfer due to modality mismatches. To bridge this gap, our work introduces a novel adversarial attack framework tailored for RES models, which—by jointly optimizing visual and textual perturbations—systematically investigates the robustness of RES models under diverse language inputs. This represents the first comprehensive study on adversarial robustness in RES tasks and provides new insights into the security of multimodal systems.

### 3. Preliminary

#### 3.1. Referring Expression Segmentation

RES is a fine-grained multimodal task that aims to segment the image region corresponding to a given natural language query. Given an input image  $x_v \in \mathbb{R}^{H \times W \times 3}$  and a textual inputs  $x_t$ , an RES model  $f(\cdot)$  outputs a predicted segmentation mask  $M_{pred} \in \mathbb{R}^{H \times W}$ , where each value indicates the confidence that a pixel belongs to the referred object:

$$M_{pred} = f(x_v, x_t). \quad (1)$$

Higher values in  $M_{pred}$  indicate a higher likelihood of inclusion in the segmented region. RES models leverage vision-language pretraining techniques and large-scale backbones, such as EVF-SAM [4] and Gres [6], enabling them to perform robustly across diverse linguistic expressions. However, this multimodal nature also introduces new vulnerabilities when subjected to adversarial perturbations.

#### 3.2. Adversarial Attacks

Adversarial attacks are designed to intentionally manipulate model outputs by introducing carefully crafted perturbations to the input data. In the context of target attacks, attackers aims to steer the model’s prediction toward a specific target output, rather than merely causing misclassification.

Formally, given a clean input  $x$  and a target output  $\mathcal{Y}_{target}$ , the objective of a targeted attack is to find an adversarial perturbation  $\delta$  such that the model prediction  $f(x + \delta)$  closely approximates the predefined target  $\mathcal{Y}_{target}$ , while keeping the perturbation magnitude imperceptibly small. This can be formulated as the following constrained optimization problem:

$$\delta^* = \underset{\delta}{\operatorname{argmin}} \mathcal{L}(f(x), \mathcal{Y}_{target}), \text{ s.t. } \|(x + \delta) - x\|_{\infty} \leq \epsilon, \quad (2)$$

where  $\mathcal{L}(\cdot)$  denotes a task-specific loss function (e.g., segmentation loss), and  $\epsilon$  is the perturbation budget that bounds the maximum allowed deviation in each pixel. This formulation ensures that the adversarial input  $x + \delta$  remains visually similar to the original  $x$ , while forcing the model output toward the target label  $\mathcal{Y}_{target}$ .

In this work, we adopt this targeted attack setting to mislead RES models, with the goal of driving the predicted mask toward a predefined target (e.g., a full background), thereby effectively suppressing the model’s segmentation ability in a controlled manner.

### 3.3. Problem Formulation

Let  $f(x_v, x_t)$  denote a pretrained RES model. Given a clean image  $x_v$  and a textual input  $x_t$ , we seek to generate a visual modality perturbation  $\delta_v$ , along with textual modality perturbation  $\delta_t$ , such that the resulting prediction  $M'_{pred}$  aligns with a predefined target mask  $M_{target}$ , such as an all-black (background-only) mask:

$$M'_{pred} = f(x_v + \delta_v, x_t + \delta_t) \approx M_{target}. \quad (3)$$

The optimization goal is to ensure that the adversarial image misleads the model under a range of text inputs, revealing its vulnerability in cross-modal reasoning scenarios.

## 4. Method

In this section, we introduce the threat model and our detailed attack method. We start with a basic single-text attack setting, then extend it to a Multi-Text attack. Finally, we leverage bidirectional adversarial optimization attacks to further enhance cross-text transferability.

### 4.1. Basic Attack Strategies: Single and Multi-Text Attacks

A straightforward strategy for generating adversarial examples against RES models involves optimizing image perturbations under the guidance of a single textual input; this approach is referred to as *Single-Text*. Building upon this, to further enhance the cross-text transferability of perturbations, a direct approach is to utilize multiple textual inputs when updating image perturbations, which is referred to as *Multi-Text*.

Let  $\mathcal{X}_t = \{x_t^1, x_t^2, \dots, x_t^K\}$  denote the set of textual inputs instances. The objective of the attack is to generate a visual perturbation  $\delta_v$  based on these textual inputs to ensure that, for single or multiple data pairs from  $\mathcal{X}_t$ , the model produces the predefined target mask  $M_{target}$ . This optimization can be mathematically represented as:

$$\min_{\delta_v} \sum_{k=1}^K \mathcal{L}_{seg}(f(x_v + \delta_v, x_t^k), M_{target}). \quad (4)$$

The distinction between *Single-Text* and *Multi-Text* lies in whether  $K$  equals 1. Specifically, in the *Single-Text* setting, the perturbation is optimized using a single textual input ( $K = 1$ ), whereas in the *Multi-Text* setting, the optimization is performed across multiple textual inputs ( $K > 1$ ), with the aim of enhancing the cross-text transferability of the adversarial perturbation.

However, we find that adversarial examples generated by this basic attack method are still likely to be correctly segmented by the model when encountering unseen textual inputs. Essentially, these basic attack methods tend to overfit the textual inputs involved in the adversarial example generation process.

### 4.2. Multimodal Bidirectional Attack(MBA)

To alleviate the problem of overfitting to proxy texts during adversarial example generation and to enhance the transferability of adversarial images under diverse textual inputs, we propose a novel attack framework called **Multimodal Bidirectional Attack(MBA)**. Grounded in the inherently multimodal structure of RES models, our method introduces a cooperative optimization strategy that simultaneously performs *visual-aligned optimization* for the visual modality and *textual-adversarial optimization* for the textual modality within a unified framework. Specifically, MBA consists of two complementary branches: the **Visual-Aligned Optimization** branch aims to minimize the discrepancy between the model’s predicted mask and a predefined target mask, thereby progressively aligning the image perturbation with the desired segmentation region; the **Textual-Adversarial Optimization** branch maximizes the loss with

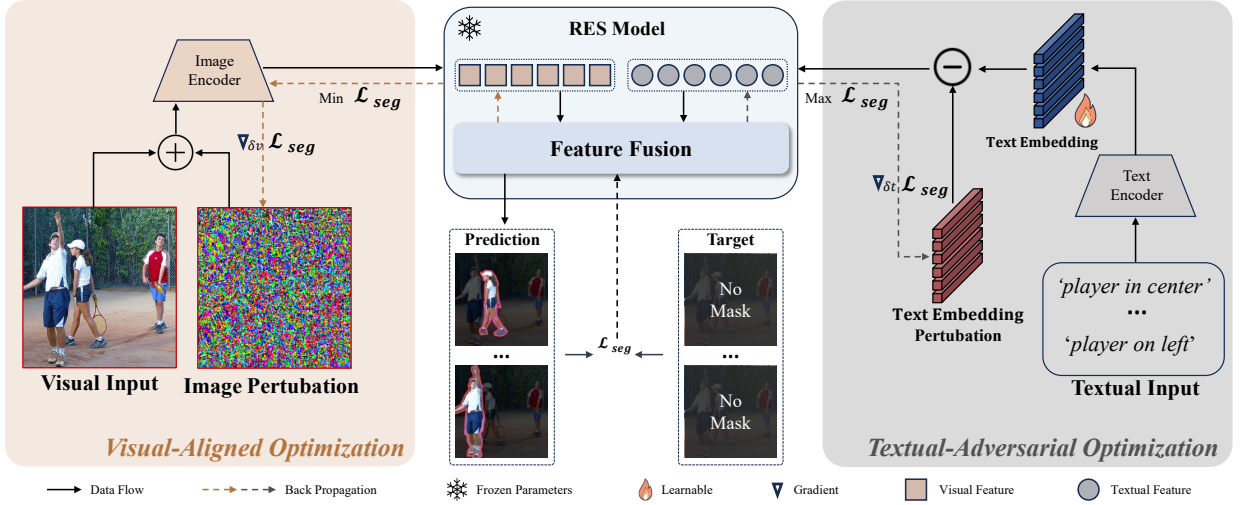


Figure 3: Overview of MBA framework. Both the image perturbation  $\delta_v$  and the text perturbation  $\delta_t$  are learnable, but the prompt perturbation does not collaborate with  $\delta_t$  to deceive the model. They are optimised with opposite goals:  $\delta_v$  aims to minimise the mask loss, while  $\delta_t$  aims to maximise the mask loss. The update frequency of the image perturbation and prompt perturbation can be different.

respect to the learnable proxy text embedding, simulating the diversity and adversarial nature of varying textual inputs to ensure that the adversarial image remains effective even when queried with previously unseen referring expressions. By alternately optimizing both the visual and textual modalities in each iteration, this bidirectional strategy enables perturbations to be collaboratively refined in the joint vision-language semantic space, ultimately yielding adversarial images that demonstrate both high generalization ability and strong attack effectiveness under different text inputs. The implementation details of each component will be elaborated in the following sections.

#### 4.2.1. Visual-Aligned Optimization

In the *Visual-Aligned Optimization* phase, our primary objective is to iteratively update the adversarial image so that the output mask produced by the RES model, given a set of textual inputs, closely aligns with a predefined target mask such as a fully black background. This phase is conceptually consistent with adversarial optimization in single- or Multi-Text settings.

Specifically, while keeping the textual inputs fixed, we perform gradient-based optimization on the image to minimize the segmentation loss between the predicted mask and the target mask  $M_{target}$ . The update rule for the adversarial image  $x'_v$  at iteration  $i + 1$  is defined as:

$$x'_v{}^{(i+1)} = \Pi_{\epsilon_v, x_v} \left( x'_v{}^{(i)} - \alpha_v \cdot \text{sign} \left( \nabla_{x_v} \sum_{k=1}^K \mathcal{L}_{seg} (f(x'_v{}^{(i)}, x_t^{(k)}), M_{target}) \right) \right), \quad (5)$$

Where  $\Pi_{\epsilon_v, x_v}(\cdot)$  denotes a projection operation that ensures the updated image remains within an  $\epsilon_v$ -bounded neighborhood of the original clean image  $x_v$ ;  $\alpha_v$  is the visual perturbation step size;  $\mathcal{L}_{seg}(\cdot)$  represents the segmentation loss function, and  $\{x_t^{(k)}\}_{k=1}^K$  denotes a set of  $k$  textual inputs. The gradient is aggregated over all texts to encourage visual perturbations that are semantically aligned across diverse textual inputs.

The resulting visual perturbation  $\delta_v$  can be expressed as:

$$\delta_v^{(i)} = \alpha_v \cdot \text{sign} \left( \nabla_{x_v} \sum_{k=1}^K \mathcal{L}_{seg} (f(x'_v{}^{(i)}, x_t^{(k)}), M_{target}) \right). \quad (6)$$

This process can be viewed as a minimization objective over the visual modality:

---

**Algorithm 1** MBA: Multimodal Bidirectional Attack
 

---

**Require:** RES Model  $f$ , Target Mask  $M_{target}$ , vision input  $x_v$ , text input  $x_t^k \in$  proxy text set  $\mathcal{X}_t = \{x_t^1, x_t^2, \dots, x_t^k\}$ , image perturbation budget  $\epsilon_v$ , proxy text embedding perturbation budget  $\epsilon_t$ , step size of images perturbation updating  $\alpha_v$ , step size of proxy text embedding perturbation updating  $\alpha_t$ , number of iteration steps  $I$ , proxy adversarial text embedding update interval  $N$

**Ensure:** Adversarial image  $x'_v$

- 1: Initialize adversarial image:  $x'_v = x_v$
  - 2: Initialize adversarial text embedding:
  - 3: **for**  $k = 1$  to  $K$  **do**
  - 4:    $\widetilde{\mathbf{E}}_{x_t^k}^k = \text{Text Encoder}(x_t^k)$
  - 5: **end for**
  - 6: **for** step = 1 to  $I$  **do**
  - 7:   Compute gradient for adversarial image:  $g_v = \nabla_{x_v} \sum_{k=1}^K \mathcal{L}_{seg}(f(x'_v, \widetilde{\mathbf{E}}_{x_t^k}^k), M_{target})$
  - 8:   Update with gradient descent:  $x'_v = x'_v - \alpha_v \cdot \text{sign}(g_v)$
  - 9:   **if** mod(step,  $N$ ) == 0 **then**
  - 10:     **for**  $k = 1$  to  $K$  **do**
  - 11:       Compute gradient for adversarial proxy texts:  $g_{\mathbf{E}_{x_t^k}^k} = \nabla_{\mathbf{E}_{x_t^k}^k} \mathcal{L}_{seg}(f(x'_v, \widetilde{\mathbf{E}}_{x_t^k}^k), M_{target})$
  - 12:       Update with gradient ascent:  $\widetilde{\mathbf{E}}_{x_t^k}^k = \widetilde{\mathbf{E}}_{x_t^k}^k + \alpha_t \cdot \text{sign}(g_{\mathbf{E}_{x_t^k}^k})$
  - 13:       Project  $\widetilde{\mathbf{E}}_{x_t^k}^k$  to be within the  $\epsilon_t$ -ball of  $\mathbf{E}_{x_t^k}^k$ :  $\widetilde{\mathbf{E}}_{x_t^k}^k = \Pi_{\epsilon_t, \mathbf{E}_{x_t^k}^k}(\widetilde{\mathbf{E}}_{x_t^k}^k)$
  - 14:     **end for**
  - 15:   **end if**
  - 16:   Project  $x'_v$  to be within the  $\epsilon_v$ -ball of  $x_v$ :  $x'_v = \Pi_{\epsilon_v, x_v}(x'_v)$
  - 17: **end for**
  - 18: **return**  $x'_v$
- 

$$\min_{\delta_v} \sum_{k=1}^K \mathcal{L}_{seg} \left( f \left( x_v + \delta_v, x_t^{(k)} \right), M_{target} \right). \quad (7)$$

This optimization strategy progressively aligns the visual perturbation  $\delta_v$  with the semantic structure of the target mask, thereby enabling the adversarial image to achieve strong attack efficacy under fixed textual inputs. Such alignment in the visual modality serves as a solid foundation for the subsequent adversarial optimization within the language modality.

#### 4.2.2. Textual-Adversarial Optimization

To further enhance the cross-text transferability of adversarial examples, we propose a textual-adversarial optimization strategy. Unlike the visual modality, which operates in a continuous space, textual inputs are inherently discrete sequences, making it impossible to directly backpropagate gradients through the original tokenized input. To address this challenge, we introduce a learnable proxy text embedding perturbation  $\mathcal{P}_{\delta_t}$ , applied to the text embedding space. This proxy serves as a continuous surrogate for discrete textual inputs, enabling gradient-based optimization during training. It is important to emphasize that  $\mathcal{P}_{\delta_t}$  is only used in the optimization phase and is not part of the final adversarial inputs that guide the optimization of transferable visual perturbations.

The objective of this optimization branch is to maximize the segmentation loss between the model’s predicted mask and a predefined target mask (e.g., an all-black background) by perturbing the text embedding. By periodically updating the embedding using adversarial noise, we mitigate overfitting to fixed training-time textual inputs and simulate broader, more diverse real-world queries. This encourages the generation of adversarial images that remain effective even when evaluated on unseen referring expressions.

The update rule for the adversarial text embedding  $\widetilde{\mathbf{E}}_{x_t^k}^{(i+1)}$  of the  $k^{\text{th}}$  textual input at iteration  $i + 1$  is defined as:

$$\widetilde{\mathbf{E}}_{x_t^k}^{(i+1)} = \Pi_{\epsilon_t, \mathbf{E}_{x_t^k}} \left( \widetilde{\mathbf{E}}_{x_t^k}^{(i)} + \alpha_t \cdot \text{sign} \left( \nabla_{\mathbf{E}_{x_t^k}^{(i)}} \mathcal{L}_{seg} \left( f \left( x_v, \widetilde{\mathbf{E}}_{x_t^k}^{(i)} \right), M_{target} \right) \right) \right), \quad (8)$$

Where  $\alpha_t$  is the update step size for the proxy text embedding perturbation, and  $\Pi_{\epsilon_t, \mathbf{E}_{x_t^k}}(\cdot)$  denotes the projection operator that constrains the adversarial embedding within an  $\epsilon_t$ -bounded  $\ell_\infty$  ball around the original clean embedding. To simulate textual inputs uncertainty, we apply a structured perturbation  $\mathcal{P}_{\delta_t}^{(i,t)}$  to corresponding  $\widetilde{\mathbf{E}}_{x_t^k}^{(i,t)}$  as follows:

$$\mathcal{P}_{\delta_t}^{(k,i)} = \alpha_t \cdot \text{sign} \left( \nabla_{\mathbf{E}_{x_t^k}^{(i)}} \mathcal{L}_{seg} \left( f \left( x_v, \mathbf{E}_{x_t^k}^{(i)} \right), M_{target} \right) \right). \quad (9)$$

This formulation explicitly pushes the embedding toward adversarial directions, thereby promoting the visual perturbation’s robustness across a wide spectrum of textual inputs. Overall, the process can be viewed as solving the following maximization objective:

$$\max_{\mathcal{P}_{\delta_t}} \sum_{k=1}^K \mathcal{L}_{seg} \left( f \left( x_v, \mathbf{E}_{x_t}^{(k)} + \mathcal{P}_{\delta_t}^{(k)} \right), M_{target} \right). \quad (10)$$

Through this textual-adversarial optimization branch, we implement a modality-specific adversarial intervention that enhances the generalization of adversarial images to diverse textual inputs. When integrated with the Visual-Aligned Optimization branch, this strategy constitutes a cohesive and effective framework (MBA) for generating highly transferable and semantically robust adversarial examples across modalities and texts.

#### 4.2.3. Multimodal Bidirectional Attack

To jointly optimize perturbations from both the visual and textual modalities, we propose a unified optimization attack strategy termed **Multimodal Bidirectional Attack**. This strategy integrates the *Visual-Aligned Optimization* and *Textual-Adversarial Optimization* branches into a single iterative framework, with the goal of generating high-quality adversarial images that not only conform to the desired target mask but also maintain transferability across diverse textual inputs. The overall pipeline of our framework is illustrated in Figure 3. The full optimization algorithm is detailed in Algorithm 1.

During each iteration of the MBA framework, we first fix the textual input and perform gradient-based updates on the image to optimize the visual perturbation  $\delta_v$ , minimizing the segmentation loss between the predicted segmentation mask and a predefined target mask (e.g., an all-black background). This alignment-oriented optimization ensures that the adversarial image drives the model prediction toward the desired attack objective.

Subsequently, we periodically activate the text-side adversarial process to update the learnable proxy text embedding perturbation  $\mathcal{P}_{\delta_t}$ . The goal of this adversarial-oriented optimization is to maximize the segmentation loss between the model prediction and the target mask, thereby challenging the visual input under varying textual inputs. By adversarially modifying the proxy embedding, we simulate diverse textual inputs and encourage the visual perturbation to remain effective under unseen textual inputs.

A critical component in this dual optimization is the update frequency of the text embedding perturbation. If updated too frequently, it may degrade the overall attack performance by interfering with visual alignment. If updated too infrequently, it may fail to simulate sufficient variability in textual inputs, thereby impairing the cross-text transferability of the adversarial examples. To balance this trade-off between attack strength and cross-text transferability, we execute one textual adversarial update every  $N$  visual step. We empirically study the influence of  $N$  in Section 5.3.2.

By alternately updating both modalities, MBA facilitates the exploration of robust adversarial directions within the joint vision-language space. This results in adversarial images that consistently mislead RES models across a wide spectrum of referring expressions, revealing critical vulnerabilities in their multimodal reasoning capabilities.

The overall optimization is formulated as a min-max process:

$$\min_{\delta_v} \max_{\mathcal{P}_{\delta_t}} \mathcal{L}_{seg} \left( f \left( x_v + \delta_v, \mathbf{E}_{x_t} + \mathcal{P}_{\delta_t} \cdot \mathbb{I}_{i \bmod N=0} \right), M_{target} \right), \quad (11)$$

where the indicator function  $\mathbb{I}_{i \bmod N=0}$  controls the periodicity of text perturbation updates to maintain the stability of image optimization while still ensuring generalization across textual inputs. This dual optimization strategy ultimately enables robust, transferable adversarial attacks tailored for multimodal segmentation systems.

#### 4.3. Loss Function

In SAM-based RES models [31], the SAM [21] outputs positive values for foreground pixels and negative values for background pixels. Following the loss function formulation in [18], we omit gradient computation for pixels that are already predicted as negative. Instead, we focus on those pixels predicted with positive values. The loss function for SAM-based RES models is defined as follows:

$$\mathcal{L}_{seg}(f(x_v, x_t), M_{target}) = \|Clip(f(x_v, x_t), min = Neg_{th}) - Neg_{th}\|^2, \quad (12)$$

where  $\mathcal{L}$  represents the Mean Squared Error (MSE) loss function, and *Clip* ensures that pixels with values lower than the threshold  $Neg_{th}$  have zero gradients. This is because computing gradients for pixels that are already not segmented is meaningless. Following attack-SAM, we set  $Neg_{th}$  to -10. In non-SAM-based RES models, we adopt the cross-entropy loss function used during model [48] training as the attack loss function. The weight of the cross-entropy loss remains the same as that used in the model [48] training process, specifically set to (0.9, 1.1). The loss function for non-SAM-based RES models is defined as follows:

$$\mathcal{L}_{seg}(f(x_v, x_t), M_{target}) = \sum_i w_i \cdot \mathcal{L}_{CE}(f(x_v, x_t), M_{target}), \quad (13)$$

Where  $i$  represents the predicted class of the model, with 0 denoting the background and 1 denoting the foreground.  $w_i$  is the weight for class  $i$ , which follows the model [48] training settings:  $w_0 = 0.9$  for the background and  $w_1 = 1.1$  for the foreground.

## 5. Experiment

### 5.1. Experiment Setup

**Datasets.** In this experiment, we evaluate our proposed attack method on three benchmark datasets: RefCOCO [49], RefCOCO+ [50], and RefCOCOg [51]. These datasets are widely used for referring expression comprehension tasks and contain a large number of image-text pairs, where each referring expression is designed to identify a specific target object in the image. Specifically, RefCOCO is derived from the MSCOCO [52] dataset and consists of 142,209 referring expressions across 50,000 images. The dataset was collected in an interactive setting, resulting in relatively short and concise expressions. RefCOCO+ is similar to RefCOCO, but the queries do not include absolute positional terms, such as specifying an object’s location as ”on the right” within the image. RefCOCOg, on the other hand, contains longer and more descriptive expressions, making it suitable for evaluating more complex vision-language understanding tasks. We utilize these datasets, each possessing distinct characteristics, to assess the effectiveness and generalizability of our proposed adversarial attack method. Specifically, we randomly select 750 images from each dataset for evaluation. To comprehensively evaluate the attack transferability across different textual inputs, we divide the dataset into the optimization phase and the evaluation phase. Specifically, for each image in the dataset, one referring expression per target object is randomly selected as the proxy textual input for optimizing adversarial perturbations. Since the number of target objects varies across images, the number of optimization texts also differs. The remaining referring expressions are used in the evaluation phase, ensuring that the optimization and evaluation phases utilize completely different textual inputs. This setup effectively assesses the cross-text transferability of the adversarial attack. In our experiments, the ratio of optimization phase texts to evaluation phase texts is approximately 1:4.

**Metrics.** To comprehensively evaluate the effectiveness of the proposed adversarial attack method, we employ the following three key metrics: **Attack Success Rate (ASR, %)**. The ASR measures the impact of adversarial samples on the model’s segmentation results. Specifically, we define ASR as the ratio of the number of pixels in the segmentation mask by adversarial image to the number of pixels in the ground truth mask. Since our objective is to make the model segment as little as possible, this ratio should be minimized. If the ratio falls below a predefined threshold, the attack is considered successful. ASR is the most critical evaluation metric in this study, as it directly reflects the effectiveness of the adversarial attack. **Mean Intersection over Union with Ground Truth (mIoU-GT, %)** mIoU-GT quantifies the similarity between the predicted segmentation mask after adversarial perturbation and the ground truth mask. This metric follows the standard IoU computation, which is the intersection area between the predicted and ground truth masks divided by their union area. A lower mIoU-GT value indicates that the predicted mask deviates more from the ground truth mask, implying a stronger attack effect. **Mean Intersection over Union between Unsegmented Regions and Target Mask (mIoU-UTM, %)**. mIoU-UTM evaluates how well the unsegmented regions in the predicted mask align with a predefined target mask, which is configured as a completely black background. In this setting, an ideal adversarial attack should prevent the model from segmenting any objects. The metric computes the IoU between the regions not covered by the predicted mask (i.e., the background) and the target mask. A higher mIoU-UTM value indicates that the unsegmented area more closely matches the target, reflecting a stronger attack that effectively suppresses the model’s segmentation capability. By leveraging these multiple evaluation metrics, we

Model	Method	RefCOCO			RefCOCOg			RefCOCO+		
		ASR@30↑	mIoU-GT↓	mIoU-UTM↑	ASR@30↑	mIoU-GT↓	mIoU-UTM↑	ASR@30↑	mIoU-GT↓	mIoU-UTM↑
EVF-SAM	Attack-SAM	5.43	76.99	88.95	1.65	68.85	91.51	1.11	72.89	92.03
	SRA	5.98	74.96	89.25	1.57	67.57	91.79	1.19	71.23	92.29
	Single-Text	36.61	40.17	93.79	19.07	48.65	93.04	18.43	50.22	93.75
	Multi-Text	81.72	10.79	98.49	77.00	12.47	98.25	75.26	14.61	98.41
	SegPGD-Single	34.76	41.57	93.68	18.66	48.46	93.23	17.42	50.84	93.76
	SegPGD-Multi	45.14	28.44	<b>98.70</b>	44.42	26.10	96.29	40.07	28.94	96.45
	<b>Ours</b>	<b>84.06</b>	<b>9.85</b>	98.65	<b>79.12</b>	<b>11.27</b>	<b>98.41</b>	<b>77.12</b>	<b>13.43</b>	<b>98.52</b>
EVF-SAM2	Attack-SAM	0.79	77.13	88.72	2.13	71.19	91.23	1.60	73.82	91.80
	SRA	0.68	77.72	88.78	1.46	72.07	91.17	1.01	74.45	91.81
	Single-Text	15.97	60.45	91.44	12.00	61.25	92.48	10.25	64.23	92.86
	Multi-Text	26.39	47.29	94.01	23.97	45.62	94.87	25.01	47.05	95.22
	SegPGD-Single	16.89	60.19	91.61	12.04	61.37	92.40	10.49	64.65	92.89
	SegPGD-Multi	26.18	42.89	93.55	28.68	37.21	94.69	26.46	40.33	94.76
	<b>Ours</b>	<b>34.55</b>	<b>40.92</b>	<b>94.53</b>	<b>32.65</b>	<b>35.35</b>	<b>95.71</b>	<b>32.54</b>	<b>36.24</b>	<b>95.75</b>
DMMI	Attack-SAM	–	–	–	–	–	–	–	–	–
	SRA	–	–	–	–	–	–	–	–	–
	Single-Text	43.07	23.89	94.56	27.00	29.97	94.03	35.03	16.55	95.04
	Multi-Text	65.97	11.65	97.02	57.07	13.76	97.11	64.01	8.52	97.32
	SegPGD-Single	34.38	25.72	92.16	20.75	31.20	92.22	25.94	18.01	92.29
	SegPGD-Multi	55.51	17.63	96.17	44.20	20.54	96.93	47.01	12.76	96.63
	<b>Ours</b>	<b>71.02</b>	<b>10.24</b>	<b>97.49</b>	<b>63.46</b>	<b>11.56</b>	<b>97.68</b>	<b>70.14</b>	<b>7.26</b>	<b>97.75</b>

Table 1: Quantitative comparison of different adversarial attack methods on three RES models (EVF-SAM, EVF-SAM2, and DMMI) across three datasets (RefCOCO, RefCOCOg, RefCOCO+). Evaluation metrics include Attack Success Rate at threshold 30 (ASR@30), foreground mIoU (mIoU-GT), and background mIoU (mIoU-UTM). ↑ indicates higher is better, and ↓ indicates lower is better.

comprehensively analyze and validate the effectiveness and generalizability of the proposed method across different datasets and models.

**Baseline.** Since there is currently no dedicated adversarial attack research targeting RES models, we adapt existing adversarial attack methods for segmentation models to fit RES models. For SAM-based RES models (EVF-SAM, EVF-SAM2), we select Attack-SAM [18], SRA [19], SegPGD-Single, SegPGD-Multi, Single-Text, and Multi-Text as baseline methods. Notably, since Attack-SAM and SRA generate adversarial samples based on SAM’s point prompt mechanism, they are not applicable to non-SAM RES models such as DMMI and are thus excluded from comparisons on DMMI. Specifically, SegPGD-Single employs a single textual input to guide the SegPGD [12] algorithm in optimizing adversarial samples, while SegPGD-Multi leverages multiple textual inputs for optimization. Single-Text and SegPGD-Single share the same proxy textual input with identical numbers. Similarly, Multi-Text, SegPGD-Multi, and our proposed method all utilize multiple proxy textual prompts during optimization, ensuring that they use the same textual inputs and maintain consistency in the number of texts for a fair comparison.

**Models.** We conduct experiments on three representative RES models: EVF-SAM [31], EVF-SAM2 [31], and DMMI [48]. These models reflect state-of-the-art architectures in RES tasks, incorporating strong multimodal encoders and text-guided mask decoders. To comprehensively evaluate adversarial robustness, we adopt a white-box attack setting across all models, where full access to the model architecture and parameters is assumed.

**Implementation.** All experiments are performed on an NVIDIA A100 GPU to ensure computational efficiency and scalability. Adversarial images are generated by applying perturbations to both the visual input and the proxy text embeddings. For the visual modality, the perturbation step size is set to  $2/255$ , with a maximum  $\ell_\infty$  constraint of  $16/255$ . For the textual modality, the perturbation is applied directly to the proxy text embeddings with a step size of 0.01 and a maximum budget of 0.2. The choice of textual modality perturbation step size is empirically validated in the ablation studies presented in Section 5.3.3. This dual-modality perturbation strategy ensures that the generated adversarial examples remain effective under diverse textual inputs, enhancing their cross-text transferability.

## 5.2. Qualitative and Quantitative Results

A comprehensive evaluation of the proposed method is conducted through detailed comparative experiments under white-box attack scenarios across three RES models: EVF-SAM, EVF-SAM2, and DMMI. Our approach was systematically compared with all previous methods listed in the table. We selected 750 images from three widely used multimodal datasets (RefCOCO, RefCOCO+, and RefCOCOg) for evaluation, covering various scenarios close

Method	$\epsilon_r = 4/255$			$\epsilon_r = 8/255$			$\epsilon_r = 12/255$			$\epsilon_r = 16/255$		
	ASR@30 $\uparrow$	mIoU-GT $\downarrow$	mIoU-UTM $\uparrow$	ASR@30 $\uparrow$	mIoU-GT $\downarrow$	mIoU-UTM $\uparrow$	ASR@30 $\uparrow$	mIoU-GT $\downarrow$	mIoU-UTM $\uparrow$	ASR@30 $\uparrow$	mIoU-GT $\downarrow$	mIoU-UTM $\uparrow$
Single-Text	5.95	54.74	92.23	15.18	43.84	93.08	23.36	35.40	93.81	26.01	30.95	94.09
Multi-Text	9.13	46.49	93.60	27.60	29.87	95.10	44.92	18.65	96.45	57.06	13.86	97.26
SegPGD-Single	3.93	55.66	91.99	11.25	42.59	92.60	14.86	35.41	92.44	22.08	31.51	92.38
SegPGD-Multi	8.59	45.81	94.28	29.19	30.33	96.03	38.75	24.22	96.57	45.22	20.59	96.97
Ours	<b>10.83</b>	<b>45.04</b>	<b>95.51</b>	<b>30.57</b>	<b>26.99</b>	<b>95.73</b>	<b>48.41</b>	<b>18.58</b>	<b>96.84</b>	<b>63.46</b>	<b>11.56</b>	<b>97.68</b>

Table 2: Performance under different perturbation budgets. For each  $\epsilon_r$ , we report ASR@30 (% $\uparrow$ ), mIoU-FG (% $\downarrow$ ), and mIoU-BG (% $\uparrow$ ). Our method consistently outperforms all baselines across various perturbation strengths.

to real-world conditions. In total, our evaluation involved more than 50,000 referring expressions, providing a large-scale and statistically significant experimental basis to ensure the reliability and credibility of the results.

Table 1 summarizes the performance of different methods on the RefCOCO, RefCOCOg, and RefCOCO+ datasets, evaluated by three key metrics: Attack Success Rate at 30% threshold (ASR@30), mean Intersection over Union for ground truth (mIoU-GT), and mean Intersection over Union between Unsegmented Regions and Target Mask (mIoU-UTM). Compared with existing baselines, our proposed method achieves significant improvements across all datasets and all evaluation metrics, particularly excelling in ASR@30, which is a critical indicator of attack effectiveness. These results clearly demonstrate that our method substantially reduces the mIoU-GT while effectively increasing the mIoU-UTM, thereby severely disrupting the model’s segmentation performance. The improvement in mIoU-UTM indicates an expansion of unsegmented regions, suggesting that the model is more likely to predict the predefined target mask (i.e., a fully black mask).

Specifically, *Multi-Text* and *SegPGD-Multi* achieve relatively better performance compared to *Single-Text* and *SegPGD-Single*, benefiting from the use of multiple textual inputs during optimization. However, these methods still suffer from varying degrees of overfitting and demonstrate limited attack effectiveness under more challenging settings. Moreover, our experimental results indicate that SegPGD, despite its effectiveness on conventional segmentation models, exhibits limited applicability to RES tasks due to the unique challenges posed by multimodal interactions. In comparison, *SRA* and *Attack-SAM*, which generate adversarial examples based on point prompts, perform poorly under natural language queries and fail to transfer to RES models. This ineffectiveness stems from the inherent modality mismatch between point-based attacks and text-guided segmentation frameworks, where the absence of language-conditioned reasoning prevents these methods from influencing the model’s language-vision alignment mechanisms. This further validates the superiority of our proposed method in RES adversarial attack scenarios. In summary, through extensive analysis utilizing multiple metrics across different models and datasets, these experimental results clearly validate the effectiveness and generalizability of our approach in cross-text adversarial attacks, highlighting its practical value and theoretical contributions.

Although our method achieves the highest ASR@30 on EVF-SAM, the mIoU-UTM value appears slightly lower than that of SegPGD-Multi. This is due to the nature of the mIoU-UTM metric, which evaluates the overlap between the unsegmented regions and the target mask (i.e., a full background). Since the background region typically occupies a large portion of the image, even small segmented areas can lead to noticeable drops in mIoU-UTM, making the numerical gap less meaningful when ASR is already high. Furthermore, across all three datasets, we observe that attack performance generally declines on EVF-SAM2. This can be attributed to the structural design of SAM2, which incorporates a memory mechanism that reinforces predictions using historical visual and prompt embeddings. This additional temporal-consistency component increases the model’s resilience to adversarial perturbations, making EVF-SAM2 inherently more robust and thus harder to attack.

A further evaluation of the cross-text generalization capability of adversarial examples is conducted through qualitative comparisons, as shown in Figure 4. We visualize the segmentation results of different attack methods under a variety of unseen textual inputs. As shown, text-guided single-text methods such as *Single-Text* and *SegPGD-Single* exhibit limited transferability: they are often only effective against a specific expression and fail to generalize to other textual inputs. While Multi-Text methods like *Multi-Text* and *SegPGD-Multi* show improved performance on some expressions, they still tend to overfit the textual inputs used during optimization, resulting in inconsistent effectiveness on unseen textual inputs. In contrast, our method consistently generates adversarial examples that yield minimal mask predictions across all referring expressions. This indicates a stronger ability to transfer across unseen textual inputs and demonstrates that our optimization strategy effectively prevents overfitting to the proxy textual inputs.

To further evaluate the stability and effectiveness of the proposed method, we compare the performance of different



Figure 4: Qualitative comparison of adversarial attacks under multiple unseen referring expressions. Each column corresponds to a different textual prompt, and each row shows the segmentation results under clean inputs and different attack methods.

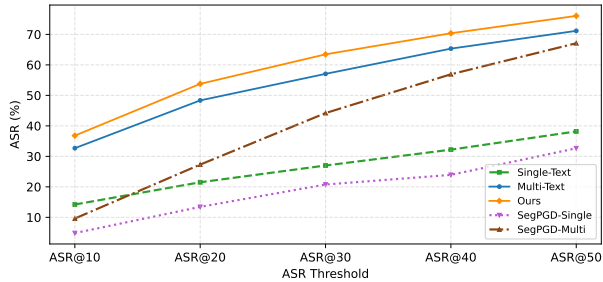


Figure 5: Attack success rates (ASR) of different methods under varying ASR thresholds (ASR@10–ASR@50). Our method consistently achieves the highest ASR across all thresholds.

approaches under various attack settings. As shown in Table 2, we report the attack success rates (ASR) under different perturbation budgets  $\epsilon_r$  (4/255, 8/255, 12/255, and 16/255). It can be observed that although the overall ASR of all methods increases with larger perturbation magnitudes, our method consistently achieves the best performance across all perturbation levels. In particular, under smaller perturbation budgets (e.g., 4/255 and 8/255), our method still exhibits a significant advantage, indicating its ability to generate highly effective adversarial examples even with limited perturbations.

Moreover, as shown in Figure 5, we further evaluate the attack performance under different ASR thresholds (ASR@10, ASR@20, ASR@30, ASR@40, and ASR@50) to assess the robustness of each method under varying tolerance levels. The results demonstrate that our method consistently maintains the highest attack success rate across all thresholds. Notably, while *Multi-Text* and *SegPGD-Multi* show a steady increase in ASR as the threshold loosens, they still fall short compared to our method, especially in more challenging scenarios with stricter thresholds. These results collectively validate the robustness and superior cross-text transferability of our approach in adversarial attack settings for RES models.

Overall, both qualitative and quantitative results consistently demonstrate the effectiveness of our method. Our method not only generates highly transferable adversarial examples across diverse unseen textual inputs but also maintains strong attack performance under varying perturbation and evaluation conditions.

### 5.3. Ablation Study

#### 5.3.1. Effect of proxy text embedding Perturbation Update Location

We investigate the optimal perturbation update locations for the MBA by designing three different update strategies on the SAM-based RES models: 1) updating only the prompt embedding in the SAM Prompt Encoder (Prompt Embedding Update, PEU); 2) simultaneously updating both the text embedding and visual inputs in the multimodal encoder (Multimodal Input Update, MIU); 3) updating only the text embedding without modifying the visual inputs (Text Embedding Update, TEU).

It is worth noting that since SAM-based RES models such as EVF-SAM and EVF-SAM2 have distinct architectures that include both a SAM Prompt Encoder and a multimodal encoder, unlike general RES models, we conduct this ablation study exclusively on SAM-based models to comprehensively analyze the impact of different update locations on attack performance.

As shown in Table 3, we evaluate the three update strategies on EVF-SAM and EVF-SAM2. Experimental results demonstrate that for EVF-SAM, updating perturbations on the prompt embedding (PEU) achieves the best performance, reaching an ASR@30 of 84.06%, with the lowest foreground mIoU-FG of 9.85, misleading that the model fails to segment the correct target regions. In contrast, both MIU and TEU strategies lead to lower attack success rates.

Interestingly, for EVF-SAM2, the optimal results are achieved under the MIU setting, where perturbations are applied simultaneously to both textual and visual inputs. Under this strategy, the ASR@30 reaches 34.55%, significantly higher than that achieved by TEU alone. This observation may be attributed to differences in the feature fusion mechanisms between EVF-SAM and EVF-SAM2, where updating only the text embedding is insufficient to effectively disrupt the final segmentation outputs.

Model	PEU	MIU	TEU	ASR@30↑	mIoU-GT↓	mIoU-UTM↑
EVF-SAM	✓			<b>84.06</b>	<b>9.85</b>	<b>98.65</b>
		✓		83.75	10.05	98.61
			✓	80.58	11.77	98.37
EVF-SAM2	✓			31.42	43.68	93.61
		✓		<b>34.55</b>	<b>40.92</b>	<b>93.92</b>
			✓	27.11	47.71	93.97

Table 3: Ablation study on update locations. PEU is best for EVF-SAM; MIU for EVF-SAM2.

Model	Metric	1	5	10	15	20
EVF-SAM	ASR@30	78.57	83.87	<b>83.99</b>	82.45	82.04
	mIoU-GT ↓	12.43	9.16	<b>9.54</b>	10.36	10.35
	mIoU-UTM ↑	98.25	98.55	<b>98.61</b>	98.48	98.44
EVF-SAM2	ASR@30	32.38	33.99	<b>34.51</b>	33.23	32.84
	mIoU-GT ↓	41.52	41.00	<b>40.95</b>	41.84	41.92
	mIoU-UTM ↑	93.98	94.48	<b>94.50</b>	93.59	93.32
DMMI	ASR@30	68.94	70.44	<b>70.96</b>	70.56	70.10
	mIoU-GT ↓	12.35	12.13	<b>10.28</b>	12.03	10.98
	mIoU-UTM ↑	95.21	95.89	<b>97.36</b>	97.29	96.73

Table 4: Ablation study on proxy text embedding perturbation update interval  $N$ . Best results occur at  $N = 10$ .

Model	Metric	0.01	0.02	0.03	0.04	0.05
EVF-SAM	ASR@30	<b>84.06</b>	83.76	82.02	80.64	79.17
	mIoU-GT ↓	<b>9.85</b>	9.55	10.83	11.25	12.87
	mIoU-UTM ↑	<b>98.65</b>	98.61	97.22	97.99	98.22
EVF-SAM2	ASR@30	<b>34.55</b>	32.94	32.13	31.99	31.42
	mIoU-GT ↓	<b>40.92</b>	42.15	41.23	43.11	43.68
	mIoU-UTM ↑	<b>94.53</b>	93.78	94.16	94.59	93.63
DMMI	ASR@30	<b>71.02</b>	70.57	69.58	69.12	67.64
	mIoU-GT ↓	<b>10.24</b>	11.46	11.99	11.23	15.35
	mIoU-UTM ↑	<b>97.49</b>	97.12	96.26	97.03	95.33

Table 5: Ablation study on step size  $\alpha_t$  for proxy text embedding perturbation. Best results occur at  $\alpha_t = 0.01$ .

Overall, these findings suggest that selecting appropriate perturbation update locations according to model architectures is crucial for maximizing cross-text transferability in adversarial attacks.

### 5.3.2. Effect of Perturbation Update Interval

We conduct an ablation study to examine how varying the update interval  $N$  for proxy text embedding perturbation influences the performance of adversarial example generation. Specifically, in our optimization process, proxy text embedding perturbations are not updated at every iteration, but rather after every  $N$  step. We evaluate the attack success rate (ASR@30) under different values of  $N \in \{1, 5, 10, 15, 20\}$  while keeping all other configurations fixed.

As shown in Table 4, the ASR initially increases with larger update intervals and reaches the peak at  $N = 10$ , achieving an ASR@30 of 83.99%, 34.51%, 70.96%. Compared to updating perturbations at every iteration ( $N = 1$ ), this setting improves the success rate by over 5%, indicating a significant performance gain. We hypothesize that a moderate update interval helps alleviate overfitting to the proxy prompts during training and promotes better semantic generalization of the adversarial perturbations. In contrast, overly frequent updates may cause the attack to overfit the gradients of a specific prompt, while overly sparse updates can reduce the effectiveness of optimization.

Therefore, we adopt  $N = 10$  as the default configuration in all subsequent experiments to strike a balance between robustness and effectiveness.

### 5.3.3. Effect of proxy text embedding Perturbation Step Size

We also analyze how the step size  $\alpha_t$  used for optimizing text embedding affects the attack results. Since each image is optimized for only 10 iterations, we fix the perturbation budget to a constant (0.2) and focus solely on the effect of step size.

Table 5 shows that the highest ASR@30 (84.06%, 34.55%, 71.02%) is achieved when  $\alpha_t = 0.01$ . Larger step sizes tend to result in unstable optimization and lower attack performance. This result suggests that smaller and more stable updates are preferable in the limited-step adversarial optimization setting.

These ablation results collectively validate the effectiveness of our proposed design choices in enhancing attack success and cross-prompt generalization. They further highlight the importance of precise update locations, appropriately spaced optimization intervals, and well-tuned step sizes in adversarial optimization for RES models.

## 6. Conclusion

In this paper, we conducted a systematic investigation into the adversarial robustness of RES models, a critical yet underexplored area in multimodal vision-language understanding. To address the unique challenge posed by the multimodal nature of RES models, we proposed a novel attack framework, *Multimodal Bidirectional Attack (MBA)*, which jointly optimizes adversarial perturbations in both visual and textual modalities. Specifically, MBA performs visual-aligned optimization to align adversarial images with a predefined target mask, while simultaneously employing textual-adversarial optimization to enhance the semantic challenge of proxy text embedding. This bidirectional

design encourages the generation of adversarial examples that remain effective across diverse textual inputs. Extensive experiments on multiple representative RES models and benchmark datasets demonstrate that our approach significantly outperforms existing baselines across various metrics, including ASR, mIoU-GT, and mIoU-UTM. We also provide qualitative visualizations showing the effectiveness of our attacks on unseen text queries, and ablation studies further confirm the necessity and impact of each component within the proposed framework. Our work not only offers new insights into the vulnerability of RES models under adversarial conditions but also lays the foundation for developing safer and more robust multimodal systems. Future research could extend this line of work by exploring transferable attacks under black-box settings and designing interpretable and controllable defense mechanisms.

## References

- [1] K. He, G. Gkioxari, P. Dollár, R. Girshick, Mask r-cnn, in: Proceedings of the IEEE international conference on computer vision, 2017, pp. 2961–2969.
- [2] J. Long, E. Shelhamer, T. Darrell, Fully convolutional networks for semantic segmentation, in: Proceedings of the IEEE conference on computer vision and pattern recognition, 2015, pp. 3431–3440.
- [3] L.-C. Chen, G. Papandreou, I. Kokkinos, K. Murphy, A. L. Yuille, Deeplab: Semantic image segmentation with deep convolutional nets, atrous convolution, and fully connected crfs, *IEEE transactions on pattern analysis and machine intelligence* 40 (4) (2017) 834–848.
- [4] H. Ding, C. Liu, S. Wang, X. Jiang, Vision-language transformer and query generation for referring segmentation, in: Proceedings of the IEEE/CVF international conference on computer vision, 2021, pp. 16321–16330.
- [5] Z. Yang, J. Wang, Y. Tang, K. Chen, H. Zhao, P. H. Torr, Lavt: Language-aware vision transformer for referring image segmentation, in: Proceedings of the IEEE/CVF conference on computer vision and pattern recognition, 2022, pp. 18155–18165.
- [6] C. Liu, H. Ding, X. Jiang, Gres: Generalized referring expression segmentation, in: Proceedings of the IEEE/CVF conference on computer vision and pattern recognition, 2023, pp. 23592–23601.
- [7] Y. Wu, Z. Zhang, C. Xie, F. Zhu, R. Zhao, Advancing referring expression segmentation beyond single image, in: Proceedings of the IEEE/CVF International Conference on Computer Vision, 2023, pp. 2628–2638.
- [8] C. Wu, Y. Liu, J. Ji, Y. Ma, H. Wang, G. Luo, H. Ding, X. Sun, R. Ji, 3d-gres: Generalized 3d referring expression segmentation, in: Proceedings of the 32nd ACM International Conference on Multimedia, 2024, pp. 7852–7861.
- [9] G. Luo, Y. Zhou, X. Sun, L. Cao, C. Wu, C. Deng, R. Ji, Multi-task collaborative network for joint referring expression comprehension and segmentation, in: Proceedings of the IEEE/CVF Conference on computer vision and pattern recognition, 2020, pp. 10034–10043.
- [10] I. J. Goodfellow, J. Shlens, C. Szegedy, Explaining and harnessing adversarial examples, arXiv preprint arXiv:1412.6572 (2014).
- [11] A. Madry, A. Makelov, L. Schmidt, D. Tsipras, A. Vladu, Towards deep learning models resistant to adversarial attacks, arXiv preprint arXiv:1706.06083 (2017).
- [12] J. Gu, H. Zhao, V. Tresp, P. H. Torr, Segpgd: An effective and efficient adversarial attack for evaluating and boosting segmentation robustness, in: European Conference on Computer Vision, Springer, 2022, pp. 308–325.
- [13] X. Jia, J. Gu, Y. Huang, S. Qin, Q. Guo, Y. Liu, X. Cao, Transegpgd: Improving transferability of adversarial examples on semantic segmentation, arXiv preprint arXiv:2312.02207 (2023).
- [14] O. Ronneberger, P. Fischer, T. Brox, U-net: Convolutional networks for biomedical image segmentation, in: Medical image computing and computer-assisted intervention—MICCAI 2015: 18th international conference, Munich, Germany, October 5–9, 2015, proceedings, part III 18, Springer, 2015, pp. 234–241.
- [15] S. Agnihotri, S. Jung, M. Keuper, Cospgd: an efficient white-box adversarial attack for pixel-wise prediction tasks, arXiv preprint arXiv:2302.02213 (2023).
- [16] X. Xu, H. Zhao, J. Jia, Dynamic divide-and-conquer adversarial training for robust semantic segmentation, in: Proceedings of the IEEE/CVF International Conference on Computer Vision, 2021, pp. 7486–7495.
- [17] C. Xie, J. Wang, Z. Zhang, Y. Zhou, L. Xie, A. Yuille, Adversarial examples for semantic segmentation and object detection, in: Proceedings of the IEEE international conference on computer vision, 2017, pp. 1369–1378.
- [18] C. Zhang, C. Zhang, T. Kang, D. Kim, S.-H. Bae, I. S. Kweon, Attack-sam: Towards evaluating adversarial robustness of segment anything model, arXiv preprint arXiv:2305.00866 1 (3) (2023) 5.
- [19] Y. Shen, Z. Li, G. Wang, Practical region-level attack against segment anything models, in: Proceedings of the IEEE/CVF Conference on Computer Vision and Pattern Recognition, 2024, pp. 194–203.
- [20] Z. Zhang, Y. Ma, E. Zhang, X. Bai, Psalm: Pixelwise segmentation with large multi-modal model, in: European Conference on Computer Vision, Springer, 2024, pp. 74–91.
- [21] A. Kirillov, E. Mintun, N. Ravi, H. Mao, C. Rolland, L. Gustafson, T. Xiao, S. Whitehead, A. C. Berg, W.-Y. Lo, et al., Segment anything, in: Proceedings of the IEEE/CVF international conference on computer vision, 2023, pp. 4015–4026.
- [22] A. Dosovitskiy, L. Beyer, A. Kolesnikov, D. Weissenborn, X. Zhai, T. Unterthiner, M. Dehghani, M. Minderer, G. Heigold, S. Gelly, et al., An image is worth 16x16 words: Transformers for image recognition at scale, in: International Conference on Learning Representations, 2020.
- [23] R. Hu, M. Rohrbach, T. Darrell, Segmentation from natural language expressions, in: Computer Vision—ECCV 2016: 14th European Conference, Amsterdam, The Netherlands, October 11–14, 2016, Proceedings, Part I 14, Springer, 2016, pp. 108–124.
- [24] R. Hu, M. Rohrbach, T. Darrell, Segmentation from natural language expressions, in: Computer Vision—ECCV 2016: 14th European Conference, Amsterdam, The Netherlands, October 11–14, 2016, Proceedings, Part I 14, Springer, 2016, pp. 108–124.
- [25] L.-C. Chen, G. Papandreou, F. Schroff, H. Adam, Rethinking atrous convolution for semantic image segmentation, arXiv preprint arXiv:1706.05587 (2017).
- [26] E. Margffoy-Tuay, J. C. Pérez, E. Botero, P. Arbeláez, Dynamic multimodal instance segmentation guided by natural language queries, in: Proceedings of the European Conference on Computer Vision (ECCV), 2018, pp. 630–645.

- [27] S. Yang, G. Li, Y. Yu, Graph-structured referring expression reasoning in the wild, in: Proceedings of the IEEE/CVF conference on computer vision and pattern recognition, 2020, pp. 9952–9961.
- [28] Z. Qian, Y. Ma, J. Ji, X. Sun, X-refseg3d: Enhancing referring 3d instance segmentation via structured cross-modal graph neural networks, in: Proceedings of the AAAI Conference on Artificial Intelligence, Vol. 38, 2024, pp. 4551–4559.
- [29] J. Wang, J. Ke, H.-H. Shuai, Y.-H. Li, W.-H. Cheng, Referring expression comprehension via enhanced cross-modal graph attention networks, *ACM Transactions on Multimedia Computing, Communications and Applications* 19 (2) (2023) 1–21.
- [30] A. Radford, J. W. Kim, C. Hallacy, A. Ramesh, G. Goh, S. Agarwal, G. Sastry, A. Askell, P. Mishkin, J. Clark, et al., Learning transferable visual models from natural language supervision, in: International conference on machine learning, PmLR, 2021, pp. 8748–8763.
- [31] Y. Zhang, T. Cheng, L. Zhu, R. Hu, L. Liu, H. Liu, L. Ran, X. Chen, W. Liu, X. Wang, Evf-sam: Early vision-language fusion for text-prompted segment anything model, arXiv preprint arXiv:2406.20076 (2024).
- [32] W. Wang, H. Bao, L. Dong, J. Bjorck, Z. Peng, Q. Liu, K. Aggarwal, O. K. Mohammed, S. Singhal, S. Som, et al., Image as a foreign language: Beit pretraining for vision and vision-language tasks, in: Proceedings of the IEEE/CVF Conference on Computer Vision and Pattern Recognition, 2023, pp. 19175–19186.
- [33] J. Bai, S. Bai, S. Yang, S. Wang, S. Tan, P. Wang, J. Lin, C. Zhou, J. Zhou, Qwen-vl: A frontier large vision-language model with versatile abilities, arXiv preprint arXiv:2308.12966 1 (2) (2023) 3.
- [34] H. Liu, C. Li, Q. Wu, Y. J. Lee, Visual instruction tuning, *Advances in neural information processing systems* 36 (2023) 34892–34916.
- [35] J. Li, D. Li, C. Xiong, S. Hoi, Blip: Bootstrapping language-image pre-training for unified vision-language understanding and generation, in: International conference on machine learning, PMLR, 2022, pp. 12888–12900.
- [36] J. Li, D. Li, S. Savarese, S. Hoi, Blip-2: Bootstrapping language-image pre-training with frozen image encoders and large language models, in: International conference on machine learning, PMLR, 2023, pp. 19730–19742.
- [37] Y.-C. Chen, W.-H. Li, C. Sun, Y.-C. F. Wang, C.-S. Chen, Sam4mllm: Enhance multi-modal large language model for referring expression segmentation, in: European Conference on Computer Vision, Springer, 2024, pp. 323–340.
- [38] X. Lai, Z. Tian, Y. Chen, Y. Li, Y. Yuan, S. Liu, J. Jia, Lisa: Reasoning segmentation via large language model, in: Proceedings of the IEEE/CVF Conference on Computer Vision and Pattern Recognition, 2024, pp. 9579–9589.
- [39] M. Siam, M. Gamal, M. Abdel-Razek, S. Yogamani, M. Jagersand, H. Zhang, A comparative study of real-time semantic segmentation for autonomous driving, in: Proceedings of the IEEE conference on computer vision and pattern recognition workshops, 2018, pp. 587–597.
- [40] L. Chen, P. Bentley, K. Mori, K. Misawa, M. Fujiwara, D. Rueckert, Drinet for medical image segmentation, *IEEE transactions on medical imaging* 37 (11) (2018) 2453–2462.
- [41] N. Papernot, P. McDaniel, I. Goodfellow, Transferability in machine learning: from phenomena to black-box attacks using adversarial samples, arXiv preprint arXiv:1605.07277 (2016).
- [42] N. Papernot, P. McDaniel, I. Goodfellow, S. Jha, Z. B. Celik, A. Swami, Practical black-box attacks against machine learning, in: Proceedings of the 2017 ACM on Asia conference on computer and communications security, 2017, pp. 506–519.
- [43] N. Inkawhich, W. Wen, H. H. Li, Y. Chen, Feature space perturbations yield more transferable adversarial examples, in: Proceedings of the IEEE/CVF Conference on Computer Vision and Pattern Recognition, 2019, pp. 7066–7074.
- [44] S. Kullback, R. A. Leibler, On information and sufficiency, *The annals of mathematical statistics* 22 (1) (1951) 79–86.
- [45] F. Croce, N. D. Singh, M. Hein, Robust semantic segmentation: Strong adversarial attacks and fast training of robust models, in: The Second Workshop on New Frontiers in Adversarial Machine Learning, 2023.
- [46] J. Rony, J.-C. Pesquet, I. Ben Ayed, Proximal splitting adversarial attack for semantic segmentation, in: Proceedings of the IEEE/CVF Conference on Computer Vision and Pattern Recognition, 2023, pp. 20524–20533.
- [47] K. Maag, A. Fischer, Uncertainty-weighted loss functions for improved adversarial attacks on semantic segmentation, in: Proceedings of the IEEE/CVF Winter Conference on Applications of Computer Vision, 2024, pp. 3906–3914.
- [48] Y. Hu, Q. Wang, W. Shao, E. Xie, Z. Li, J. Han, P. Luo, Beyond one-to-one: Rethinking the referring image segmentation, in: Proceedings of the IEEE/CVF International Conference on Computer Vision, 2023, pp. 4067–4077.
- [49] L. Yu, P. Poirson, S. Yang, A. C. Berg, T. L. Berg, Modeling context in referring expressions, in: Computer Vision–ECCV 2016: 14th European Conference, Amsterdam, The Netherlands, October 11–14, 2016, Proceedings, Part II 14, Springer, 2016, pp. 69–85.
- [50] S. Kazemzadeh, V. Ordonez, M. Matten, T. Berg, Referitgame: Referring to objects in photographs of natural scenes, in: Proceedings of the 2014 conference on empirical methods in natural language processing (EMNLP), 2014, pp. 787–798.
- [51] V. K. Nagaraja, V. I. Morariu, L. S. Davis, Modeling context between objects for referring expression understanding, in: Computer Vision–ECCV 2016: 14th European Conference, Amsterdam, The Netherlands, October 11–14, 2016, Proceedings, Part IV 14, Springer, 2016, pp. 792–807.
- [52] T.-Y. Lin, M. Maire, S. Belongie, J. Hays, P. Perona, D. Ramanan, P. Dollár, C. L. Zitnick, Microsoft coco: Common objects in context, in: Computer vision–ECCV 2014: 13th European conference, zurich, Switzerland, September 6–12, 2014, proceedings, part v 13, Springer, 2014, pp. 740–755.